Excited-State Dipole Moments and Transition Dipole Orientations of Rotamers of 1,2-, 1,3-, and 1,4-Dimethoxybenzene

Michael Schneider,[a] Martin Wilke,[a] Marie-Luise Hebestreit,[a] Christian Henrichs,[a] W. Leo Meerts,[b] and Michael Schmitt*[a]

Rotationally resolved electronic Stark spectra of rotamers of 1,2-, 1,3-, and 1,4-dimethoxybenzene have been recorded and analyzed using evolutionary strategies. The experimentally determined dipole moments as well as the transition dipole moments are compared to the results of ab initio calculations. For the electronic ground states of the experimentally observed dimethoxybenzenes, the permanent dipole moments can be obtained from vectorial addition of the monomethoxybenzene dipole moment. However, this is not the case for the electronically excited states. This behavior can be traced back to a state mixing of the lowest electronically excited singlet states for the asymmetric rotamers. For the symmetric rotamers however, this is not valid. We discuss several possible reasons for the non-additivity of the dipole moments in the excited states of the symmetric rotamers.

1. Introduction

The knowledge of excited-state dipole moments and of transition dipole moments are important prerequisites for the understanding of resonance energy transfer processes such as Förster resonant energy transfer (FRET)[1,2] and for molecular excitonic interactions.[3] Whereas experimental dipole moment measurements in the electronic ground state are straightforward, their exact values in electronically excited states can only be determined reliably using gas-phase spectroscopic methods. Despite numerous attempts to improve the original Lippert–Mataga theory,[4–10] for a determination of excited-state dipole moments (or at least their changes from the ground state values), the results are not very encouraging.[11–13] On the other hand, theoretical approaches frequently fail when the excited states involve considerable charge-transfer character.[14] Very subtle changes of the electron densities can change both magnitude and direction of the excited-state dipole moments considerably.

Ligands that show mesomeric (+M for electron releasing or −M for electron-withdrawing groups) effects cause large electron-density changes upon electronic excitation of the chromophore. The hydroxy or methoxy groups, for example, shift electrons into an aromatic chromophore via their +M effect.

[a] M. Schneider, Dr. M. Wilke, M.-L. Hebestreit, C. Henrichs, M. Schmitt
Heinrich-Heine-Universität Düsseldorf
Institut für Physikalische Chemie I
40225 Düsseldorf (Germany)
E-mail: mschmitt@uni-duesseldorf.de

[b] Prof. Dr. W. L. Meerts
Radboud University
Institute for Molecules and Materials, Felix Laboratory
Toernooiveld 7c, 6525 ED Nijmegen (The Netherlands)

Supporting Information and the ORCID identification number(s) for the author(s) of this article can be found under:
https://doi.org/10.1002/cphc.201701095.

This effect is substantially larger in the lowest excited singlet states of methoxy- and hydroxy-substituted benzenes,[15,16] leading to quinoidal structures upon excitation, especially in the ortho and para disubstituted conformers.[17] However, inductive (+I or −I) effects and even through-space effects also influence the electron distribution between the ligand and the chromophore. For the hydroxy and methoxy substituents, it has been found that the adjacent C-atom to which the lone pairs of the O-atom points, has the lower electron density.[18–20] Thus, it is interesting to investigate the dipole moments of different rotamers of disubstituted benzenes, which either can talk to each other electronically (ortho and para), or communicate only via inductive effects (meta).

Structural changes upon electronic excitation have been addressed by rotationally resolved electronic spectra of (mono)-methoxy substituted benzene (anisole) in the groups of Becucci[16] and Pratt,[21] and of (mono)hydroxybenzene (phenol) in the groups of Meerts[15] and Schmitt.[22] For anisole, no spectral splitting due to the hindered threefold internal rotation of the methoxy group has been observed, probably because of the high barriers for this motion.

Molecular beam R2PI spectra of 1,2-, 1,3-, and 1,4-dihydroxybenzene have been reported by Dunn et al., from which they concluded the existence of two rotamers for 1,4-dihydroxybenzene and of three rotamers for 1,2- and 1,3-dihydroxybenzene, respectively.[23] Bürgi and Leutwyler studied 1,2-dihydroxybenzene (catechol), using hole-burning spectroscopy.[24] They found, that all bands in the vibronic spectrum belong to a single rotamer. Myszkiewicz et al. presented a study on 1,3-dihydroxybenzene (resorcinol), using rotationally resolved laser-induced fluorescence spectroscopy.[25] Only two rotamers could be identified in the molecular beam spectra of 1,3-dihydroxybenzene. Two 1,4-dihydroxybenzene (benzoquinone) rotamers

have been studied at rotational resolution in the group of Pratt and the two origins were assigned to the *cis* and *trans* rotamers on the basis of their different nuclear spin statistical weights and the different rotational constants.[17]

Huang et al.[26] measured the vibrational spectrum of 1,2-dimethoxybenzene (1,2-DMB) in the S_1 and in the D_0 states and found only one conformer in the resonant two-color ionization spectrum. A high-resolution study of 1,2-DMB and its water cluster has been performed in the Pratt group.[27] They could show that all bands in the vibronic spectrum have the same rotational constants in the ground state and belong therefore to the same rotamer, which was identified from a comparison to quantum chemical calculations as the *trans*-1,2-DMB rotamer. Three bands, labeled *A*, *B*, and *C* at 36101.5, 36163.9, and 36256.9 cm^{-1} in the R2PI molecular beam spectrum of 1,3-dimethoxybenzene (1,3-DMB) have been assigned to the origins of three different rotamers by Breen et al.[28] Yang et al.[29] performed two-color resonant two-photon mass-analyzed threshold ionization spectroscopy to investigate selected rotamers of 1,2-DMB and 1,3-DMB in their ionic states. They found three different ionization potentials for the bands *A* to *C* in the R2PI spectrum of the 1,3-conformer from ref. [28] and also concluded the existence of three different rotamers. However, Schneider et al.[30] could show that the *C*-band is, in fact, not due to another rotamer, but is a vibronic transition that is built on the electronic *A* band origin. Oikawa et al.[31] and Tzeng et al.[32] investigated structures and vibrations of 1,4-dimethoxybenzene (1,4-DMB) conformers in their S_0 and S_1 states. They found two planar rotamers, which they named *cis* and *trans*. Yamamoto et al.[33] recorded the fluorescence emission spectra of both rotamers of 1,4-DMB. They found that the *cis* rotamer of 1,4-DMB selectively forms complexes with polar solvent molecules, whereas both the *cis* and the *trans* rotamer form complexes with unpolar solvent molecules.

In the following we will present a detailed study of the permanent dipole moments of several rotamers of the three isomeric DMBs in the ground and the first electronically excited singlet state and of the transition dipole moments for the transition connecting these two states.

Computational and Experimental Methods

Quantum Chemical Calculations

Structure optimizations were performed employing Dunning's correlation consistent polarized valence triple zeta (cc-pVTZ) basis set from the Turbomole library.[34, 35] The equilibrium geometries of the electronic ground and the lowest excited singlet states were optimized using the approximate coupled cluster singles and doubles model (CC2) employing the resolution-of-the-identity approximation (RI).[36–38] Anharmonic normal mode analyses have been performed to compute vibrational averaging effect on the inertial defects of the molecules under consideration. Such an anharmonic analysis is implemented in the Gaussian program package.[39] The procedure for the calculation of cubic and of some of the quartic force constants utilizes numerical derivatives of the analytically determined Hessian with respect to the normal coordinates. We performed the analysis at the MP2 level with the 6-311G(d,p) basis set.

Fits of the Rovibronic Spectra Using Evolutionary Algorithms

Evolutionary algorithms have proven to be perfect tools for the automated fit of rotationally resolved spectra, even for large molecules and dense spectra.[40–43] Beside a correct Hamiltonian to describe the spectrum and reliable intensities inside the spectrum, an appropriate search method is needed. Evolutionary strategies are powerful tools to handle complex multi-parameter optimizations and find the global optimum. For analysis of the presented high-resolution spectra we used the covariance matrix adaptation evolution strategy (CMA-ES), which is described in detail elsewhere.[44, 45] In this variant of global optimizers, mutations are adapted via a covariance matrix adaptation (CMA) mechanism to find the global minimum even on rugged search landscapes that are additionally complicated due to noise, local minima and/or sharp bends. The analysis of the rotationally resolved electronic Stark spectra is described in detail in ref. [46].

Experimental Methods

1,2-Dimethoxybenzene ($\geq$ 99%), 1,3-dimethoxybenzene (98%) and 1,4-dimethoxybenzene ($\geq$ 98%) were purchased from Sigma–Aldrich and used without further purification. The samples were heated to 60 °C (for 1,2- and 1,3-dimethoxybenzene) and 100 °C (for 1,4-dimethoxybenzene) and co-expanded with 200–300 mbar of argon into the vacuum through a 200 μm nozzle. After the expansion, a molecular beam was formed using two skimmers (1 mm and 3 mm, 330 mm apart) linearly aligned inside a differentially pumped vacuum system consisting of three vacuum chambers. The molecular beam was crossed at right angles with the laser beam 360 mm downstream of the nozzle. To create the excitation beam, 10 W of the 532 nm line of a diode-pumped solid-state laser (Spectra-Physics Millennia eV) pumped a single frequency ring dye laser (Sirah Matisse DS) operated with Rhodamine 110. The light of the dye laser was frequency doubled in an external folded ring cavity (Spectra Physics Wavetrain) with a resulting power of about 25 mW (1,2-dimethoxybenzene) and about 80 mW (1,3- and 1,4-dimethoxybenzene) during the experiments. The fluorescence of the samples was collected perpendicular to the plane defined by laser and molecular beam using an imaging optics setup consisting of a concave mirror and two plano-convex lenses onto the photocathode of a UV enhanced photomultiplier tube (Thorn EMI 9863QB). The signal output was then discriminated and digitized by a photon counter and transmitted to a PC for data recording and processing. The relative frequency was determined with a *quasi* confocal Fabry–Perot interferometer. The absolute frequency was obtained by comparing the recorded spectrum to the tabulated lines in the iodine absorption spectrum.[47] A detailed description of the experimental setup for the rotationally resolved laser induced fluorescence spectroscopy has been given previously.[48, 49]

To record rotationally resolved electronic Stark spectra, a parallel pair of electro-formed nickel wire grids (18 mesh per mm, 50 mm diameter) with a transmission of 95% in the UV was placed inside the detection volume, one above and one below the molecular beam—laser beam crossing with an effective distance of 23.49 $\pm$ 0.05 mm.[46] In this setup, the electric field is parallel to the polarization of the laser radiation. With an achromatic λ/2 plate (Bernhard Halle, 240–380 nm), mounted on a linear motion vacuum feedthrough, the polarization of the incoming laser beam can be rotated by 90° inside the vacuum.

2. Results

2.1. Computational Results

The nomenclature for the rotamers of the three isomeric dimethoxybenzenes we adopt here refers to the dihedral angles of the methoxy groups with respect to the aromatic plane. The numbering starts at the lowest number in the benzene ring, at the position adjacent to the first substituent. For the first rotamer of 1,2-DMB in Figure 1, the first dihedral angle formed by C(2)C(1)O(7)C(9) is 180°, the second by C(3)C(2)O(8)C(10) is 0°. Thus, the labeling for this rotamer is (180/0). The second rotamer has a dihedral angle C(2)C(1)O(7)C(9) of 0° and C(3)C(2)O(8)C(10) of 0°, therefore named (0/0).

The (180/0) rotamer of 1,2-DMB was optimized at the CC2//cc-pVTZ level of theory in the S_0 and the lowest excited singlet state S_1 and found to be the most stable conformer of 1,2-DMB. The Cartesian coordinates of all stable structures are given in the Supporting Information. Starting the optimization at the (0/0) geometry, the structure converges to a *gauche* rotamer with one methoxy group tilted out of the aromatic plane, while the other methoxy group stays in-plane. The energy of this rotamer is 6.2 kJ mol^{-1} higher than the lowest energy rotamer (180/0), cf. Table 1. Under molecular beam conditions, this conformer is probably not populated. Furthermore, the experimentally determined inertial defects (cf. section 2.2) prove heavy-atom planarity for all observed rotamers. Therefore, this rotamer is omitted from the further discussion. Confining the optimization of the (0/0) rotamer to a planar heavy atom arrangement, leads to a first-order transition state. For the (0/180) rotamer, the methyl groups overlap within their van der Waals radii. A structure optimization starting from this geometry converges to the most stable (180/0) rotamer.

Three 1,3-DMB rotamers, shown in the second line of Figure 1, have been found to be energetically compatible with cooling conditions in a molecular beam. The lowest energy rotamer is (0/0), followed by (180/0), which is 2.2 kJ mol^{-1} higher in energy and (0/180), which is 2.7 kJ mol^{-1} higher. All three rotamers are planar in the electronic ground state. The (0/0) and (180/0) structures are also planar in the electronically excite state, whereas the six-ring of the (0/180) rotamer is tilted considerably out-of-plane in the excited S_1-state. This nonplanarity upon electronic excitation has already been reported by Wilke et al.[30]

The smallest energetic difference between the two stable rotamers is found for 1,4-DMB. The (180/0) rotamer is more stable by 1.1 kJ mol^{-1} than the (0/0) rotamer. Also for 1,4-DMB, both rotamers have planar heavy atom structures in both electronic states.

Additionally, we calculated the dipole moments of anisole (monomethoxybenzene) at the CC2/cc-pVTZ level of theory for both electronic states. These quantities will be utilized in the following for construction of the dipole moments of the dimethoxybenzenes from vector addition arguments; they are given in Table 2.

The dipole moments in the ground and lowest excited singlet states of anisole and of the most stable rotamers of 1,2-DMB, 1,3-DMB, and 1,4-DMB are compiled in Tables 2, 3, 4, and 5. The rotamers, with the methoxy groups symmetric to the *b*-axis, have for symmetry reasons no component of the dipole moment in the *a* direction.
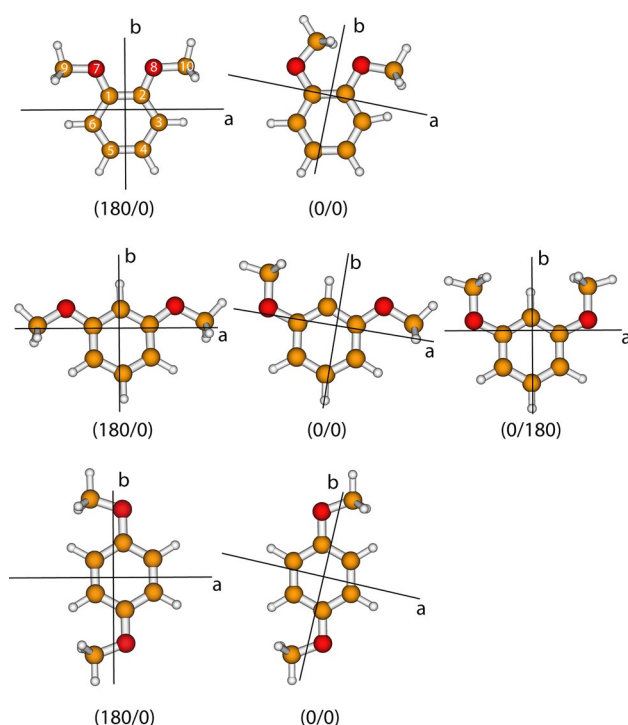

Figure 1. Structures of the rotamers of 1,2-dimethoxybenzene, 1,3-dimethoxybenzene, and 1,4-dimethoxybenzene with their principal inertial axes. The (180/180) rotamers of all three conformers are equivalent to the (0/0) rotamer. For 1,4-dimethoxybenzene, (0/180) and (180/0) are also equivalent structures. The (0/180) rotamer of 1,2-dimethoxybenzene is not a stable minimum because of steric hindrance of the neighboring methoxy groups.

Table 1. Absolute energies, zero-point vibrational energies, and relative energies including zero-point energy (ZPE) corrections of different rotamers of 1,2-, 1,3-, and 1,4-dimethoxybenzene in the electronic ground state at CC2//cc-pVTZ level of theory. The relative energies are given with respect of the most stable rotamer of each isomer.

Rotamer	1,2-DMB (180,0)	(0,0)	1,3-DMB (180,0)	(0,0)	(0,180)	1,4-DMB (180,0)	(0,0)
E_{abs} [a.u.]	−460.4062926	−460.4036199	−460.4107042	−460.4115791	−460.4105434	−460.4085741	−460.408131
ZPE [a.u.]	0.1659015	0.1655773	0.1660763	0.1660966	0.1660894	0.1658473	0.165837
E_{rel} [kJ mol^{-1}]	0.000	6.166	2.244	0.000	2.700	0.000	1.137

Table 2. Calculated rotational constants, permanent electric dipole moments μ, and their components μ_i along the main inertial axes $i = a,b,c$ of anisole compared to the respective experimental values. Doubly primed parameters belong to the electronic ground and single primed to the excited state. θ_D is the angle of the dipole moment vector with the main inertial a-axis. A positive sign of this angle means a clockwise rotation of the dipole moment vector onto the main inertial a-axis. θ is the angle of the transition dipole moment with the main inertial a-axis. A positive sign of this angle means a clockwise rotation of the dipole moment vector onto the main inertial a-axis for a molecular orientation as in Figure 1.

	Theory	Experiment
A'' [MHz]	5019	5028.84414(19)[a]
B'' [MHz]	1578	1569.364308(68)[a]
C'' [MHz]	1210	1205.825614(41)[a]
$\Delta I''$ [amu Å^2]	−3.29	−3.409
μ''_a [D]	0.58	0.69[a]
μ''_b [D]	1.20	1.05[a]
μ'' [D]	1.33	1.26[a]
θ''_D [°]	64	56.7
A' [MHz]	4773	4795.17(13)
B' [MHz]	1566	1555.68(4)
C' [MHz]	1188	1184.45(3)
$\Delta I'$ [amu Å^2]	−3.20	−3.58
μ'_a [D]	1.55	1.59(3)
μ'_b [D]	1.70	1.50(3)
μ' [D]	2.30	2.19(4)
θ'_D [°]	+48	±43.4
θ [°]	73	69.70(1)
ν_0 [cm^{-1}]	37179[b]	36384.07

[a] Set to the microwave values from Ref. [51] [b] Adiabatic excitation energy, including ZPE corrections.

2.2. Experimental Results

2.2.1. Permanent Dipole Moments and Transition Dipole Moment of Anisole

The rotationally resolved electronic spectrum of anisole (monomethoxybenzene) has been presented and analyzed before.[6,21] However, no Stark measurements have been performed until now, and the dipole moment in the excited singlet state is not known experimentally. For anisole in solution, an excited-state dipole moment from solvatochromic shifts has been reported.[50] However, agreement with gas-phase Stark data are usually bad, and the components in the inertial frame of the molecule were not given. Given that the orientation of the dipole moments in the excited state are needed in the discussion of the DMBs, we measured and analyzed the Stark spectrum of anisole (shown in Figure S1 of the Supporting Information). The dipole moments have been obtained from a combined fit to the Stark spectra in parallel as well as in perpendicular arrangement of laser polarization and electric field.[46] The fit using the CMA-ES algorithm yielded the parameters given in Table 2. The dipole components, which have been obtained by Desyatnyk et al.[51] using microwave Stark spectroscopy, have been kept fixed in our fit, due to the inherently greater accuracy of the MW values. Experimental rotational constants and dipole moments of both electronic states are in good agreement with the results for the CC2//cc-pVTZ

optimized structure. From the ratio of intensities of the a and the b lines of anisole, the angle of the TDM with the inertial a axis can be determined to be 72°, in close agreement with the theoretical value.

2.2.2. Permanent Dipole Moments and Transition Dipole Moment of 1,2-DMB

Figure 2 shows the rotationally resolved electronic spectrum of the origin band of 1,2-DMB at zero field and at a field strength of 400.24 V cm^{-1} with parallel orientation of electromagnetic and electric field ($\Delta M = 0$). The zero-field spectrum of 1,2-DMB has been measured before in the group of David Pratt and its inertial parameters are reported in Ref. [27]. The zero-field spectrum was fit using a rigid rotor Hamiltonian,[52] while the spectrum with electric field was fit using a Stark rigid rotor Hamiltonian with $\Delta M = 0$ selection rules.[46,53,54]

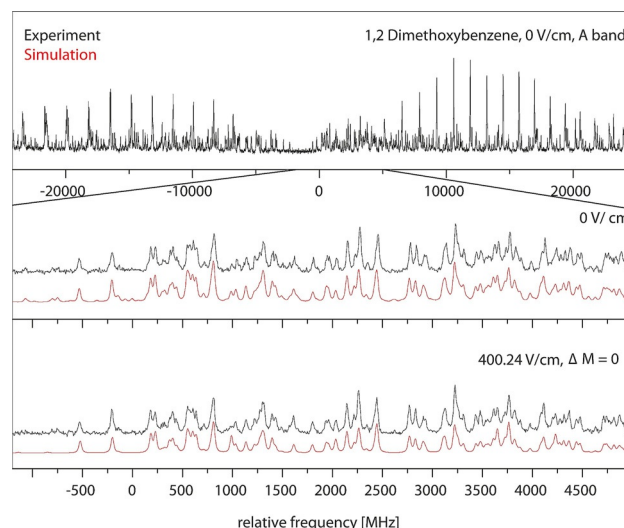The experimental rotational constants and the permanent

Figure 2. Rotationally resolved electronic spectrum of the electronic origin of the A band of 1,2-DMB at zero field and at 400.24 V cm^{-1} $\Delta M = 0$ selection rules, along with a simulation with the best CMA-ES fit parameters.

dipole moments in both electronic states, which are derived from the fit of the Stark spectrum are given in Table 3 and compared to the calculated dipole moments of both rotamers of 1,2-DMB. Both the inertial parameters and the dipole moments point to the (180/0) rotamer as being responsible for the origin band of 1,2-DMB. The small dipole moment of 0.17 D in the ground state and 0.78 D in the electronically excited state makes an angle θ_D of 90° with the inertial a-axis in both states, which means that it is oriented along the inertial b-axis of the molecule. Also the transition dipole moment is purely b-axis polarized with an angle θ of 90°. This value has already been reported by the Pratt group.[27] They presented a fit of the zero-field spectrum of 1,2-DMB with pure b-type selection rules. Thus, for 1,2-DMB, the dipole moments in both electronic states, as well as the transition dipole moment are collinear.

Table 3. Calculated rotational constants, permanent electric dipole moments μ, and their components μ_i along the main inertial axes $i = a,b,c$ of the (180/0) and the (0/0) conformers of 1,2-dimethoxybenzene compared to the respective experimental values. Doubly primed parameters belong to the electronic ground and single primed to the excited state. θ_D is the angle of the dipole moment vector with the main inertial a-axis. A positive sign of this angle means a clockwise rotation of the dipole moment vector onto the main inertial a-axis.

	Theory (180/0)	(0/0)[a]	Experiment A band
A'' [MHz]	1679	1751	1663.1(1)
B'' [MHz]	1348	1375	1349.8(1)
C'' [MHz]	755	778	752.6(1)
$\Delta I''$ [amu Å^2]	−6.40	−6.58	−6.80
μ''_a [D]	0.00	1.87	0.00
μ''_b [D]	0.05	1.42	0.17(22)
μ'' [D]	0.05	2.35	0.17(22)
θ''_D [°]	90	37	90(1)
A' [MHz]	1658	1734	1641.6(1)
B' [MHz]	1322	1369	1329.1(1)
C' [MHz]	742	773	742.7(1)
$\Delta I'$ [amu Å^2]	−6.42	−6.82	−7.68
ΔA [MHz]	−21	−17	−21.5
ΔB [MHz]	−26	−6	−20.7
ΔC [MHz]	−13	−23	−9.9
μ'_a [D]	0.00	3.48	0.00
μ'_b [D]	0.97	0.92	0.78(4)
μ' [D]	0.97	3.59	0.78(4)
θ'_D [°]	90	14	90(1)
θ [°]	90	40	90
ν_0 [cm^{-1}]	37884	35586[b]	35751

[a] First-order transition state [b] Adiabatic excitation energy, including ZPE corrections.

The CC2/cc-pVTZ calculated rotational constants of the (180/0) rotamer are in very good agreement with the experimentally determined parameters. This holds for the ground-state rotational constants, as well as for the excited state. The changes of the rotational constants upon electronic excitation are all negative and similarly small ($\Delta A = -21.5$ MHz, $\Delta B = -20.7$ MHz, $\Delta C = -9.9$ MHz).

2.2.3. Permanent Dipole Moments and Transition Dipole Moment of 1,3-DMB

Three origin bands of different rotamers of 1,3-DMB have been observed by Tzeng et al.[28] and Breen et al.[28] using resonant two-photon ionization spectroscopy and labeled A, B, and C. The zero-field spectra of these three bands of 1,3-DMB have been presented previously by Schneider et al.[30] They showed that the C band is not due to a third rotamer, but instead to a vibronic band built on the A band origin. The rotational constants for the fit of A and the B band in the two electronic states have been set fixed to the values from this publication and only the dipole moment components in both states have been fit. Figure 3 shows the rotationally resolved electronic spectrum of the A band of 1,3-DMB at zero field and at 400.24 V cm^{-1}. The zero-field and Stark spectra of the B band are shown in the Supporting Information (see Figure S2).
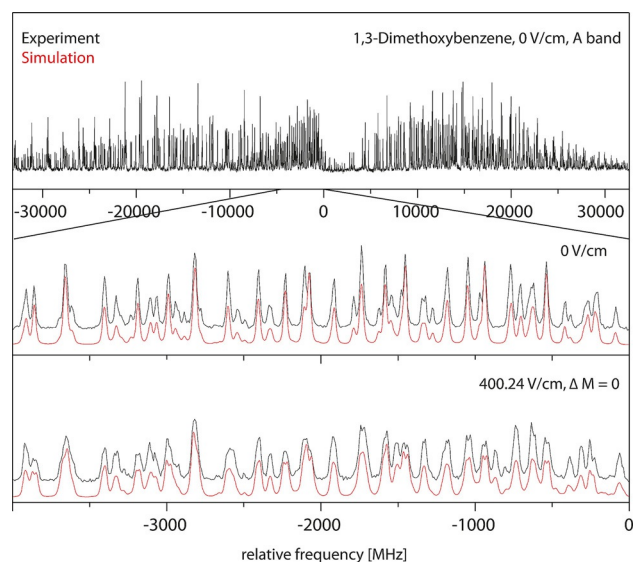

Figure 3. Rotationally resolved electronic spectrum of the electronic origin of the A band of 1,3-DMB at zero field and at 400.24 V cm^{-1} with 80% transitions of $\Delta M = 0$, along with a simulation with the best CMA-ES fit parameters.

The experimental rotational constants and the permanent dipole moments from CMA-ES fits of both bands are given in Table 4 and compared to the calculated molecular parameters of the three most stable rotamers of 1,3-DMB. From the comparison of the rotational constants it is clear that the A band belongs to the (0/0) rotamer and the B band originates from the (180/0) rotamer. Although the (0/180) rotamer is only by 2.7 kJ mol^{-1} less stable than the most stable (0/180) rotamer, it has not been observed in molecular beam experiments. This finding has been explained in a previous publication by the nonplanarity of the (0/180) rotamer in the electronically excited states, which causes a small Franck–Condon factor in the excitation spectrum.[30]

It should be noted that not only do the ground-state rotational constants of the A and the B band of 1,3-DMB allow for a straightforward assignment of the origin bands to the (0/0) and (180/0) rotamers, but also the changes of the rotational constants upon electronic excitation show very good agreement for both rotamers. Interestingly, the changes of the A rotational constants are quite different: ΔA for the (0/0) rotamer decreases by 55.79 MHz, while ΔA for the (180/0) rotamer decreases by 123.68 MHz. ΔB and ΔC are both small and negative.

The permanent dipole moment of the A band, which is assigned to the (0/0) rotamer, has components along both the a and the b inertial axes, which result in an absolute dipole moment of 1.19 D in the ground state and of 1.42 D in the excited state. The dipole moments make angles θ_D with the a axis of 15° in the electronic ground state and of 29° in the excited state. The transition dipole makes an angle θ with the a axis of 14.5°. Thus, the dipole moment and transition dipole moment have roughly the same orientation in the molecular frame.

Table 4. Summary of the CC2/cc-pVTZ calculated and experimental permanent electric dipole moments μ and their components μ_i along the main inertial axes $i = a,b,c$ of the rotamers of 1,3-dimethoxybenzene. Double primed parameters belong to the electronic ground and single primed to the excited state. Additionally the angle θ_D of the dipole moment vector with the main inertial a-axis is given.

	Theory (0/0)	(180/0)	(0/180)	Experiment A band	B band
A'' [MHz]	2539	3486	1892	2533.44(45)	3461.98(36)
B'' [MHz]	893	771	1108	887.52(2)	768.20(4)
C'' [MHz]	666	636	705	663.11(2)	634.01(4)
$\Delta I''$ [amu Å^2]	−6.40	−6.40	−6.41	−6.78	−6.74
μ''_a [D]	1.04	0.00	0.00	1.15(4)	0.00
μ''_b [D]	0.79	1.52	2.62	0.31(5)	1.66(1)
μ'' [D]	1.30	1.52	2.62	1.19(5)	1.66(1)
θ''_D [°]	37	90	90	15(3)	90(1)
A' [MHz]	2482	3358	1863	2477.65(45)	3338.30(36)
B' [MHz]	880	763	1091	875.60(3)	760.63(4)
C' [MHz]	655	626	695	652.93(3)	624.86(4)
$\Delta I'$ [amu Å^2]	−6.42	−6.42	−7.44	−7.14	−7.03
ΔA [MHz]	−57	−128	−29	−55.79	−123.68
ΔB [MHz]	−13	−8	−17	−11.92	−7.57
ΔC [MHz]	−11	−10	−10	−10.18	−9.15
μ'_a [D]	1.71	0.00	0.00	1.25(4)	0.00
μ'_b [D]	0.16	1.28	3.01	0.68(10)	1.36(1)
μ' [D]	1.72	1.28	3.01	1.42(8)	1.36(1)
θ'_D [°]	6	90	90	29(5)	90(1)
θ [°]	6	0	0	±14.5(1)	0.0[a]
ν_0 [cm^{-1}]	36809[b]	36986[b]	36455[b]	36117.61(2)	36185.72(1)

[a] For reasons of symmetry the angle was set to zero. [b] Adiabatic excitation energy, including ZPE corrections.

The permanent dipole moment of the B band, which is assigned to the (180/0) rotamer, is oriented along the inertial b axis, with a slightly smaller absolute value in the excited state (1.36 D) compared with the ground state (1.66 D). However, the transition dipole is oriented along the a axis and thus rotated by 90° with respect to the individual permanent dipole moments of both states. This surprising behavior will be explained later.

2.2.4. Permanent Dipole Moments and Transition Dipole of 1,4-DMB

1,4-DMB exists in two different stable rotamers, named A and B by Oikawa et al.,[31] equivalent to the cis and trans 1,4-dihydroxybenzene (hydroquinone) rotamers, which are, according to the above nomenclature, the (180/0) and the (0,0) rotamer, respectively. Given that the (0/0) rotamer has a center of symmetry, the resulting dipole moment should be exactly zero by symmetry arguments. The rotationally resolved zero-field electronic spectra of both rotamers have not been presented before and are used in the following to determine the inertial parameters of the two rotamers.

In a first step, the zero-field spectra of the A (cf. Figure 4) and the B (Figure S3 of the Supporting Information) bands were fit using the CMA-ES algorithm, yielding the inertial parameters in both electronic states. These are presented in Table 5, along with the results of the CC2/cc-pVTZ calculations. Comparison of the experimental and calculated rotational constants clearly shows that the A band can be assigned to the (0/0) rotamer, whereas the B band is due to the (180/0) rotamer.

For 1,2-DMB and 1,3-DMB, the changes of the rotational constants upon electronic excitation are also very well reproduced by the CC2 calculations. For both rotamers of 1,4-DMB, large negative changes of ΔA and very small changes for ΔB and ΔC are found.

Subsequently, the Stark spectra were recorded at field strengths of 400.24 V cm^{-1} and were fit using the CMA-ES algorithm (Figure 5). The spectrum of the A band does not show
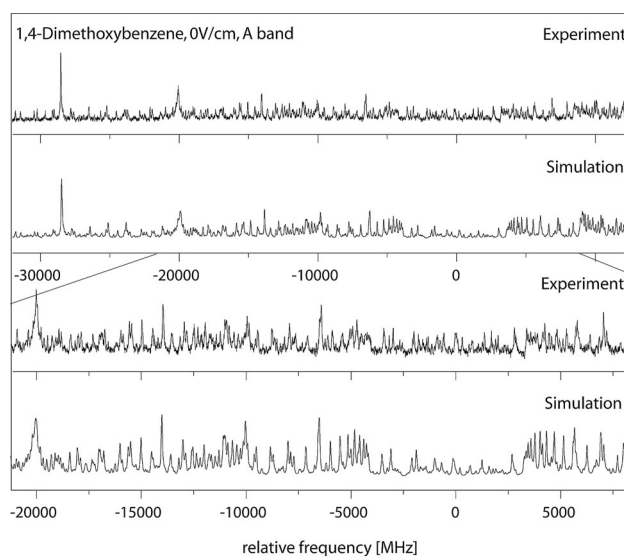

Figure 4. Rotationally resolved spectrum of the electronic origin of the A band of 1,4-dimethoxybenzene, along with a simulation using the best CMA-ES fit parameters.

Table 5. Molecular parameters of the two rotamers of 1,4-dimethoxybenzene from a CMA-ES fit of the electronic zero-field spectra. The angle of the transition dipole moment with the main inertial a-axis is given by θ and the adiabatic excitation energy by v_0.

| | Theory | | Experiment | |
	(0/0)	(180/0)	A band	B band
A'' [MHz]	4477	3963	4494.55(20)	3995.84(8)
B'' [MHz]	699	721	693.99(4)	714.52(2)
C'' [MHz]	609	615	606.26(4)	611.23(2)
$\Delta I''$ [amu Å²]	−6.40	−6.39	−7.07	−6.96
μ''_a [D]	0.00	0.00	0.00(10)	0.00[a]
μ''_b [D]	0.00	2.24	0.00(10)	2.23(1)
μ'' [D]	0.00	2.24	0.00(14)	2.23(1)
θ''_D [°]	−	90	−	90(1)
A' [MHz]	4294	3794	4319.35(36)	3835.76(11)
B' [MHz]	701	724	695.47(5)	716.68(3)
C' [MHz]	607	613	604.18(5)	609.05(3)
$\Delta I'$ [amu Å²]	−6.42	−6.43	−7.21	−7.14
ΔA [MHz]	−183	−169	−175.2	−160.08
ΔB [MHz]	+2	+3	+1.48	+2.16
ΔC [MHz]	−2	−2	−2.08	−2.18
μ'_a [D]	0.00	0.00	0.00	0.00[a]
μ'_b [D]	0.00	2.92	0.00	2.76(1)
μ' [D]	0.00	2.92	0.00	2.76(1)
θ'_D [°]	−	90	−	90(1)
θ [°]	81	90	71.91(1)	90.00
τ [ns]	−	−	2.58(1)	2.64(1)
v_0 [cm⁻¹]	33674[b]	33945[b]	33629.66(21)	33849.63(11)

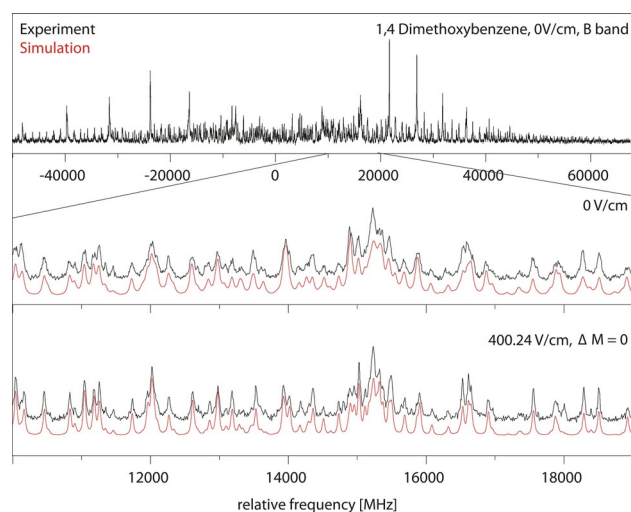[a] Fixed to zero for symmetry reason. [b] Adiabatic excitation energy, including ZPE corrections.

Figure 5. Rotationally resolved electronic spectrum of the electronic origin of the B band of 1,4-DMB at zero field and at 400.24 V cm⁻¹ with 80 % transitions of $\Delta M = 0$, along with a simulation with the best CMA-ES fit parameters.

line splitting or shifts, and for the permanent dipole moment in both states we determine an upper limit of 0.1 D for the individual components and 0.14 D for the absolute value in both states. The B band, which is due to the (180/0) rotamer, has a dipole moment along the inertial b axis of 2.76 D.

3. Discussion

3.1. Permanent Dipole Moments

3.1.1. Ground State

The molecular dipole moments of the three isomeric DMBs in their electronic ground states can be derived from simple vector addition models. Each of the DMB dipole moments can be thought of as a sum of two individual anisole dipole moments, the orientations of which are given by the mutual orientation and the position of the two methoxy groups in the aromatic ring.

Using microwave Stark spectroscopy, the dipole moment components of anisole in the electronic ground state has been determined by Desyatnyk et al.[51] to be $\mu_a = 0.6937(12)$ D, $\mu_b = 1.0547(8)$ D from which a value of $|\mu| = 1.2623(14)$ D results for the absolute dipole moment. The dipole moment makes an angle of 56.7° with the inertial a axis of anisole (cf. Figure 6a).

Figure 6 shows the results of a vectorial addition of the dipole moments derived from anisole for the 1,2-, 1,3-, and 1,4-DMB rotamers in this study. The dipole vectors have been shifted from the anisole center of mass (COM) to the COM of the respective DMB for clarity. Figure 6a shows the dipole moment of anisole in its inertial axis frame.

For the only rotamer that was observed for 1,2-DMB (180/0), the vector addition shown in Figure 6b results in a cancelation of the a-components of the dipole moment in the ground state. Given that the angle between the two anisole dipole moment vectors is small, the resulting dipole moment is oriented along the b-axis of the molecule and is close to zero, as determined experimentally. The exact analysis yields an angle of 170° between the two vectors with a length of 1.26 D, resulting in a sum dipole moment of 0.2 D, which is close to the experimental value of 0.17 D.

Two rotamers were observed for 1,3-DMB. For the (180/0) rotamer, the two anisole dipole moments lie symmetrically about the b-axis and form an angle of 50° with the b-axis (Figure 6c). The resulting dipole moment in the b direction is 1.62 D, which is again in good agreement with the experimental value for μ_b of 1.66 D. For the (0/0) rotamer, vector addition of the two anisole dipole vectors results in a vector with both a and b components (Figure 6d). Assuming an angle between the anisole fragment dipoles of 104° (as in the (180/0) rotamer), numerical values of 1.20 D and 0.45 D for the dipole moment components are obtained, in fair agreement with the experimental values of 1.15 D for μ_a and of 0.31 D for b.

For 1,4-DMB, two rotamers have also been found experimentally. Whereas for the (0,0) rotamer no dipole moment results, due to its inversion symmetry (Figure 6f), the (180/0) rotamer shows a dipole moment in the b direction, which has the largest value of all components for the rotamers of the three DMB conformers, due to the small angle of 63° between the anisole fragment dipoles. From this angle, we calculate a resulting dipole moment of 2.24 D, in good agreement with the experimental value of 2.22 D.

Thus, for the electronic ground state, the dipole moments of all rotamers can be nicely calculated from the anisole fragment
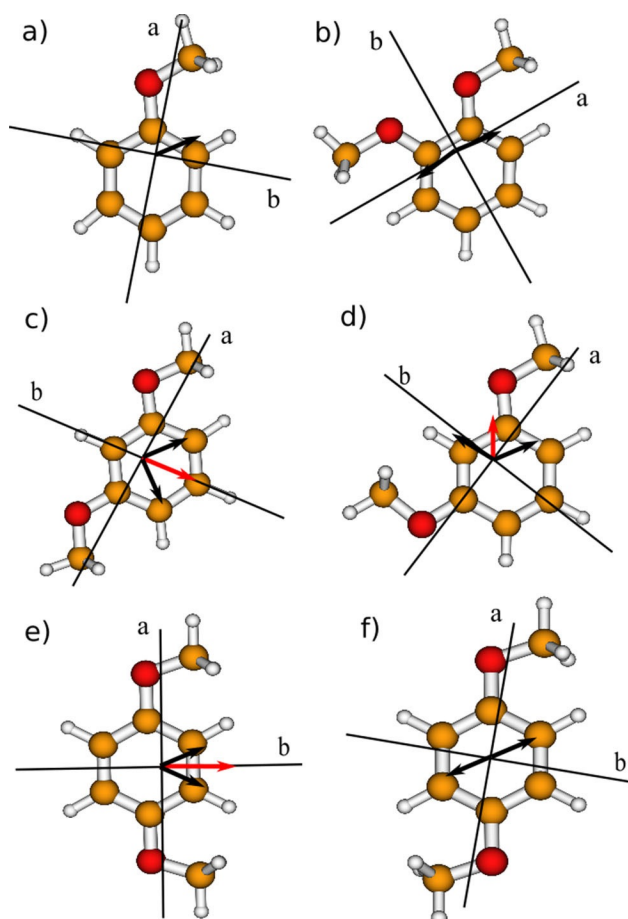
Figure 6. a) Inertial axes and ground-state dipole moment of anisole (from Ref. [51]). b) Vector addition of the experimental anisole ground-state dipole moment for (180/0)-1,2-DMB. c) Vector addition of the experimental anisole dipole moment for (180/0)-1,3-DMB. The resulting dipole moment (in red) is oriented along the *b*-axis. d) Vector addition of the experimental anisole dipole moment for (0/0)-1,3-DMB. The resulting dipole moment (in red) has components both on the *a*- and the *b*-axis. e) Vector addition of the experimental anisole dipole moment for (180/0)-1,4-DMB. The resulting dipole moment (in red) is oriented along the *b*-axis. f) Vector addition of the experimental anisole dipole moment for (0/0)-1,4-DMB. The individual dipoles cancel each other out.

dipole moments. For rotamers in which the dipole moment is oriented along one of the inertial axes, the agreement is very good, for the (0/0) rotamer of 1,3-DMB, which shows an *ab* hybrid dipole, the agreement is fair. This ground state additivity of bond dipole moments has already been shown for different conformers of aminophenol by Reese et al.[55] and for aminobenzonitrile by Borst et al.[56]

3.1.2. Excited State

In the following section, we will apply the same vector addition of bond dipole moments of anisole to the excited states of the DMBs. The resulting dipole moment components in the excited state have been determined to be $\mu_a = 1.59(3)$ D and $\mu_b = 1.50(3)$ D from which a value of $|\mu| = 2.19(4)$ D results for the absolute dipole moment (cf. Table 1). Thus, the absolute dipole moment of anisole increases by 0.93 D, and the angle

between the dipole moment vector and the inertial *a* axis changes from 56.7° to 43.4° upon electronic excitation. The orientation and absolute value of the excited state anisole dipole is shown in Figure 7 a.

For 1,2-DMB, we found that the dipole moment in the *b* direction greatly increases from 0.17 D to 0.78 D. However, this increase is not found in the vectorial addition of the anisole bond dipole moments. Figure 7 b shows the result of the vector addition with the anisole bond dipole moment added
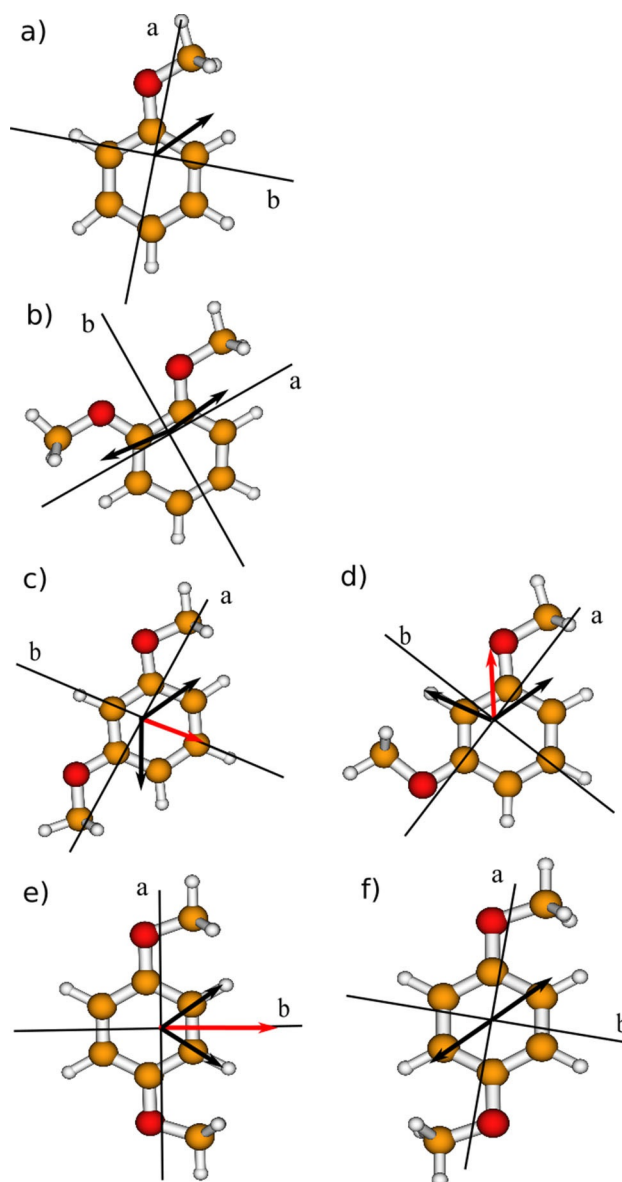

Figure 7. a) Inertial axes and excited-state dipole moment of anisole. b) Vector addition of the experimental anisole excited-state dipole moment for (180/0)-1,2-DMB. c) Vector addition of the experimental anisole dipole moment for (180/0)-1,3-DMB. The resulting dipole moment (in red) is oriented along the *b*-axis. d) Vector addition of the experimental anisole dipole moment for (0/0)-1,3-DMB. The resulting dipole moment (in red) has components both on the *a*- and the *b*-axis. e) Vector addition of the experimental anisole dipole moment for (180/0)-1,4-DMB. The resulting dipole moment (in red) is oriented along the *b*-axis. f) Vector addition of the experimental anisole dipole moment for (0/0)-1,4-DMB. The individual dipoles cancel each other out.

for each of the methoxy groups in 1,2-DMB. Although the excited-state dipole vector of anisole is larger by a factor of 1.7, the angle between the inertial a axis and the dipole moment changes by only 10°. Thus, both bond dipoles are still nearly antiparallel and almost cancel each other out.

For the (180/0) rotamer of 1,3-DMB, vectorial addition completely fails for the excited-state dipole moment. For the ground state, a permanent dipole of 1.66 D in the b direction was determined experimentally, which decreases to 1.36 D upon electronic excitation. Vector addition of the anisole dipoles, which include an angle of 100°, should lead to a value of 1.92 D (Figure 7 c); that is, an increase of 16% in spite of the experimentally determined decrease of 8%.

Finally, the same analysis for the (180/0) rotamer of 1,4-DMB leads to an excited-state dipole moment from vector addition of 3.35 D in the b direction, which is much higher than the experimentally observed value of 2.76 D (cf. Figure 7 d).

3.2. Transition Dipole Moments

We start the discussion with the cases in which dipole moments and transition dipole moment (TDM) are oriented along one of the inertial axes. The $S_1 \leftarrow S_0$ TDMs of the (180/0) rotamers of 1,2-DMB and 1,4-DMB are oriented along the inertial b-axis, as the permanent dipole moments in the ground and excited states. For the (180/0) rotamer of 1,3-DMB, the TDM is oriented along the inertial a-axis, whereas both ground- and excited-state dipole moments are oriented along the b-axis. So we have the special case in the (180/0) rotamer of 1,3-DMB, that the permanent dipole moments in both states and the transition dipole moment are perfectly perpendicular to each other. We recall the fact that the expectation value of the permanent dipole moment is defined as $< \Psi''|\hat{\mu}|\Psi'' >$ for the ground state, $< \Psi'|\hat{\mu}|\Psi' >$ for the excited state dipole moments, and $< \Psi'|\hat{\mu}|\Psi'' >$ for the transition dipole moment. Here, the Ψ'' and Ψ' are the wave functions of the ground and excited state, respectively, and $\hat{\mu}$ is the dipole operator. In other words, the transition dipoles are the off-diagonal matrix elements of the three-dimensional position operator, multiplied with the elementary charge and the permanent dipoles are the diagonal elements. For dipole moments along one axis, the question arises, if a nonzero expectation value of the dipole moment with respect to this axis defines also a nonzero expectation value of the transition dipole moment with respect to the same axis. Clearly, this is not the case for the (180/0) rotamer of 1,3-DMB. The molecular frontier orbitals and the excitations, which contribute to the $S_1 \leftarrow S_0$ transitions of the observed rotamers of the three dimethoxybenzenes are given in the Supporting Information (Figures S4–S6). For the discussion here, the relative phases of the leading contributions to the transition are sufficient. Figure 8 shows how the orientation of the TDM in the inertial axes frames can be derived from the relative phases of the MOs. The upper row of Figure 8 shows the phases of the HOMOs of the respective conformer, the second row those of the LUMOs and the third row gives the product, from which the TDM orientation results.
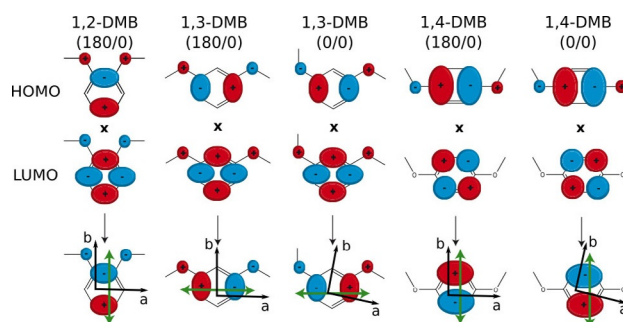

Figure 8. TDM orientations of the experimentally observed rotamers of 1,2-DMB, 1,3-DMB, and 1,4-DMB. The lowest row shows the direct product of the phases of the HOMO and the LUMO wavefunctions, the resulting TDM (in green) and the inertial axes systems.

The angles that the TDMs make with the inertial axes in the (0/0) rotamers of 1,3-DMB and of 1,4-DMB are determined only by the rotation of the inertial axis system, due to the internal rotation of one of the methoxy groups. For both the 1,3-DMB and 1,4-DMB (0/0) rotamers, the inertial axis systems are rotated by 15° with respect to the (180/0) rotamers. The experimental TDM orientation of (0/0) 1,3-DMB makes an angle of 14.5° with the a-axis, in excellent agreement with the former consideration. For (0/0) 1,4-DMB, the angle of the TDM with the a-axis is 72°, which is close to the value expected from a pure geometric axis rotation of $90° - 15° = 75°$.

The electronic character of the excited state can be described by the nodal planes of the molecular orbitals involved in the transition. According to the particle-on-a-ring model for cata-condensed hydrocarbons of Platt,[57] nodes of the MOs that bisect the bonds of benzene lead to a L_a state, whereas nodes of the MOs that go through the atoms of benzene lead to a L_b state. Heilbronner and Murrell have extended the original Platt classification of excited states for substituted benzenes, which have a C_2 symmetry axis. Here, the labels a and b distinguish the symmetry with respect to that symmetry axis, cf Figure 9.[1] States that give transitions that are parallel to the twofold axis have the label a, whereas those transitions that are perpendicular to this axis are label b.[58]

We start the discussion with the three rotamers that have a twofold symmetry axis. For the (180/0) rotamer of 1,2-DMB, the symmetry axis is the b axis, and the TDM is parallel to this axis (Figure 8). Hence, the $S_1 \leftarrow S_0$ transition of 1,2-DMB is labeled as L_a state, in agreement with the fact that the leading contribution to the $S_1 \leftarrow S_0$ transition of 1,2-DMB is LUMO←HOMO. For the (180/0) rotamer of 1,3-DMB, the symmetry axis is still the inertial b axis, but now the TDM is oriented perpendicular to that axis. Hence, the resulting excited state is an L_b state for this isomer. Finally, for the (180/0) rotamer of 1,4-DMB, the symmetry axis is the inertial b axis, which bisects the bonds of the aromatic ring in this case. The TDM is parallel to this axis, leading to an L_b state.

1 For both the odd and even-atom systems, if the molecule has a two-fold symmetry axis passing through an atom, then transitions to a states are polarized parallel to that axis, transitions to b states at right angles to this.[58]
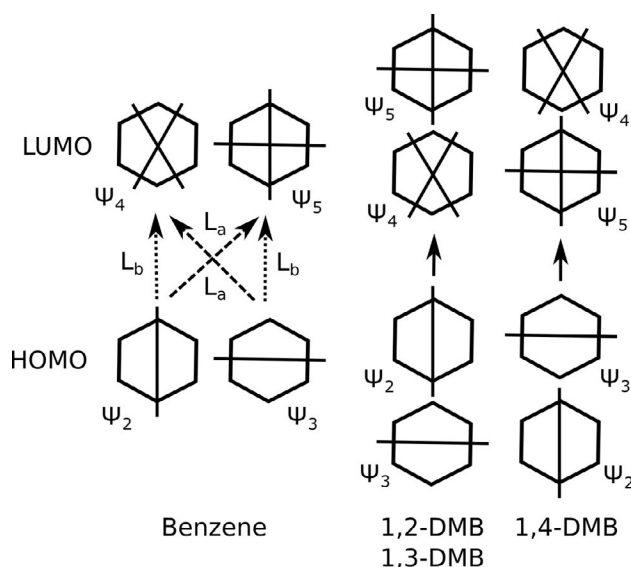
Figure 9. Nodes of the four frontier MOs for benzene and for the three symmetric DMBs. The two (degenerate) LUMO←HOMO transitions in benzene (L_a dashed lines, L_b dotted) are forbidden by symmetry. The degeneracy is lifted by the substituents in the DMBs.

These assignments are further supported by the experimentally observed changes of the rotational constants upon electronic excitation. Whereas excitation to an L_a state leads to a benzenoid distortion of the ring, excitation to the L_b state results in a quinone-like distortion. The first case will have the decrease of the rotational constants distributed evenly, whereas the L_b excitation will show a large ΔA and much smaller ΔB and ΔC. Table 6 shows exactly this behavior.

Table 6. Changes of the rotational constants upon electronic excitation. The rotamers with C_2 symmetry axis are (180/0), those without are (0/0) rotamers.

| | C_2 axis | | | no C_2 axis | |
	1,2-DMB	1,3-DMB	1,4-DMB	1,3-DMB	1,4-DMB
ΔA [MHz]	−21.5	−123.7	−160.1	−55.8	−175.2
ΔB [MHz]	−20.7	−7.6	+2.2	−11.9	+1.5
ΔC [MHz]	−9.9	−9.15	−2.2	−10.2	−2.1
state	L_a	L_b	L_b	mixed L_a/L_b	

The electronically excited states of the asymmetric (0/0) rotamer of 1,3-DMB are mixed, which can be deduced from the intermediate changes of the rotational constants (Table 6) and from the coefficients of the MOs for the excitation to the lowest singlet state (Figure S5 of the Supporting Information). Whereas all other (symmetric) rotamers have components of the excitation from HOMO to LUMO and from HOMO−1 to LUMO+1, there is some amount of HOMO−1 to LUMO excitation in this rotamer. There is surprisingly little mixing of the excited states in the asymmetric (0/0) rotamer of 1,4-DMB. Therefore, the orientation of the TDM in the molecular frame is determined by the amount the inertial axes are rotated away from the positions of the symmetric molecules.

4. Conclusions

For several rotamers of the three isomeric dimethoxybenzenes, the orientation and magnitudes of the permanent dipole moments in the ground (S_0) and lowest excited singlet (S_1) states, and the orientation of the transition dipole moment for the $S_1 \leftarrow S_0$ transition, have been determined from rotationally resolved electronic Stark spectroscopy. The orientation of the permanent dipole moments and of the transition dipole moment for excitation of the same electronically excited state of the DMB rotamers is not necessarily the same. For 1,2-DMB, the permanent dipole moments in both states and the transition dipole moment for the transition to the S_1-state are all oriented along the inertial b axis. For 1,3-DMB, the permanent dipole moments lies along the b axis, whereas the TDM for the $S_1 \leftarrow S_0$ transition is a-polarized. 1,4-DMB shows the same behavior as 1,2-DMB. All dipoles and the TDM are oriented along the inertial b axis. For the (0/0) rotamers, which do not have the TDMs oriented along one of the inertial axes, the angle of TDM with the inertial a axis is directly obtained from the rotation of the inertial axis system upon internal rotation of one of the methoxy groups by 180°; that is, the effect of the orientation of the oxygen lone pairs with respect to the chromophore is small.

For all isomers and rotamers studied here, the ground-state dipole moments of the dimethoxybenzenes can be deduced from the dipole moment of anisole by bond dipole moment vector addition. Application of vector addition rules for molecular dipole (or higher multipole) moment works in the approximation of bond dipoles, if the distribution of the electrons is localized in the regions of the bonds. This is, in general, fulfilled in the electronic ground state of a molecule. However, this is not true for the electronically excited singlet state. Such a non-additivity of bond dipole moments has been found before by Reese et al.[55] for *cis* and *trans* *m*-aminophenol. The authors assumed that the off-axis substitution in these isomers is responsible for a state mixing of S_1 and S_2 zero-order states[2]. We therefore calculated the contributions to the excitation to the S_1 and S_2 states, respectively; these are summarized in Table 7. For the symmetric (180/0) rotamers, the contributions to the excitations to the S_1 state are either HOMO−1→LUMO and HOMO→LUMO+1 with different relative phases, or nearly pure HOMO→LUMO excitations; that is, they can be described in a pure L_a or L_b scheme. The respective S_2 states have strong contributions of mixed excitations. Thus, for the S_1 state of the symmetric rotamers of DMB, there is no strong state mixing, which might be responsible for the non-additivity of the excited-state dipole moments.

It has to be mentioned that the direction of the excited state dipole moments is predicted correctly for all symmetric rotamers. Simple addition of bond dipole moments completely ignores the higher multipole expansion terms such as quadrupole moments. The CC2 calculations show that both the magnitude and the anisotropy of quadrupole moments are substantially different in both electronic states. Therefore, dipole–

---

2 The ^1L_b and ^1L_a states in the notation of Platt.[57]

CHEMPHYSCHEM
Articles

Table 7. CC2/cc-pVTZ calculated vertical excitation energies and coefficients of the contributions to the excitation to the S₁ and S₂ states.											
1,2-DMB (0/0)		(180/0)		1,3-DMB (0/0)		(180/0)		1,4-DMB (0/0)		(180/0)	
S_1	S_2	S_1	S_2	S_1	S_2	S_1	S_2	S_1	S_2	S_1	S_2
ν_{vert} 33580	33597	34805	35173	30245	30651	37503	42581	32594	33376	32992	33091
HOMO→LUMO 0.91	−0.61	–	0.85	–	0.91	–	0.91	0.60	0.74	0.95	–
HOMO−1→LUMO –	0.44	0.50	−0.21	0.87	0.21	0.85	–	0.34	−0.20	–	0.41-
HOMO−2→LUMO 0.22	–	–	0.18	–	−0.22	–	0.31	–	–	–	–
HOMO→LUMO+1 –	0.51	−0.69	0.31	−0.31	–	−0.49	–	−0.66	0.57	–	−0.86
HOMO→LUMO+2 –	–	–	–	–	−0.14	–	–	–	–	0.16	–

quadrupole interactions can also be expected to be quite different in both electronic states, leading to the observed discrepancies in the excited state. Inductive effects might also play a big role, given that the polarizability of the DMBs can be expected to be higher in the excited state compared with the ground state.

Acknowledgements

Conflict of interest

The authors declare no conflict of interest.

[1] T. Förster, *Ann. Phys.* **1948**, *437*, 55.
[2] J. Lakowicz, *Principles of Fluorescence Spectroscopy*, 2nd ed., Plenum, New York, **1999**.
[3] H. van Amerongen, L. Valkunas, R. van Grondelle, *Photosynthetic Excitons*, World Scientific Publishing, Singapore, **2000**.
[4] E. Lippert, *Z. Naturforsch. A* **1955**, *10*, 541.
[5] N. Mataga, Y. Kaifu, M. Koizumi, *Bull. Chem. Soc. Jpn.* **1956**, *29*, 465.
[6] T. Abe, *Bull. Chem. Soc. Jpn.* **1991**, *64*, 3224.
[7] P. Suppan, *J. Photochem. Photobiol. A* **1990**, *50*, 293.
[8] L. Bilot, A. Kawski, *Z. Naturforsch. A* **1962**, *17*, 621.
[9] N. Bakhshiev, *Opt. Spectrosc.* **1962**, *13*, 24.
[10] E. M. Rae, *J. Phys. Chem.* **1957**, *61*, 562.
[11] J. R. Lombardi, *J. Phys. Chem. A* **1998**, *102*, 2817.
[12] J. R. Lombardi, *J. Phys. Chem. A* **1999**, *103*, 6335.
[13] E. G. Demissie, E. T. Mengesha, G. W. Woyessa, *J. Photochem. Photobiol. A* **2017**, *337*, 184.
[14] J. J. Eriksen, S. P. Sauer, K. V. Mikkelsen, O. Christiansen, H. J. A. Jensen, J. Kongsted, *Mol. Phys.* **2013**, *111*, 1235.
[15] G. Berden, W. L. Meerts, M. Schmitt, K. Kleinermanns, *J. Chem. Phys.* **1996**, *104*, 972.
[16] C. Eisenhardt, G. Pietraperzia, M. Becucci, *Phys. Chem. Chem. Phys.* **2001**, *3*, 1407.
[17] S. J. Humphrey, D. W. Pratt, *J. Chem. Phys.* **1993**, *99*, 5078.
[18] M. Wilke, C. Brand, J. Wilke, M. Schmitt, *Phys. Chem. Chem. Phys.* **2016**, *18*, 13538.
[19] N. Schiccheri, M. Pasquini, G. Piani, G. Pietraperzia, M. Becucci, M. Biczysko, J. Bloino, V. Barone, *Phys. Chem. Chem. Phys.* **2010**, *12*, 13547.
[20] M. Wilke, M. Schneider, J. Wilke, J. Ruiz-Santoyo, J. Campos-Amador, M. Gonzléz-Medina, L. Álvarez-Valtierra, M. Schmitt, *J. Mol. Struct.* **2017**, *1140*, 59.
[21] J. W. Ribblett, W. E. Sinclair, D. R. Borst, J. T. Yi, D. W. Pratt, *J. Phys. Chem. A* **2006**, *110*, 1478.
[22] C. Ratzer, J. Küpper, D. Spangenberg, M. Schmitt, *Chem. Phys.* **2002**, *283*, 153.
[23] T. M. Dunn, R. Tembreull, D. M. Lubman, *Chem. Phys. Lett.* **1985**, *121*, 453.
[24] T. Bürgi, S. Leutwyler, *J. Chem. Phys.* **1994**, *101*, 8418.
[25] G. Myszkiewicz, W. L. Meerts, C. Ratzer, M. Schmitt, *ChemPhysChem* **2005**, *6*, 2129.
[26] J.-H. Huang, W.-B. Tzeng, K.-L. Huang, *Chin. J. Chem.* **2008**, *26*, 51.
[27] J. T. Yi, J. W. Ribblett, D. W. Pratt, *J. Phys. Chem. A* **2011**, *109*, 9456.
[28] P. J. Breen, E. R. Bernstein, H. V. Sector, J. I. Seeman, *J. Am. Chem. Soc.* **1989**, *111*, 1958.
[29] S. C. Yang, S. W. Huang, W. B. Tzeng, *J. Phys. Chem. A* **2010**, *114*, 11144.
[30] M. Schneider, M. Wilke, M.-L. Hebestreit, J. A. Ruiz-Santoyo, L. lvarez Valtierra, J. T. Yi, W. L. Meerts, D. W. Pratt, M. Schmitt, *Phys. Chem. Chem. Phys.* **2017**, *19*, 21364.
[31] A. Oikawa, H. Abe, N. Mikami, M. Ito, *Chem. Phys. Lett.* **1985**, *116*, 50.
[32] W. B. Tzeng, K. Narayanan, C. Hsieh, C. C. Tung, *J. Mol. Struct.* **1998**, *448*, 91.
[33] N. M. Seiji Yamamoto, K. Okuyama, M. Ito, *Chem. Phys. Lett.* **1986**, *125*, 1.
[34] R. Ahlrichs, M. Bär, M. Häser, H. Horn, C. Kölmel, *Chem. Phys. Lett.* **1989**, *162*, 165.
[35] J. T. H. Dunning, *J. Chem. Phys.* **1989**, *90*, 1007.
[36] C. Hättig, F. Weigend, *J. Chem. Phys.* **2000**, *113*, 5154.
[37] C. Hättig, A. Köhn, *J. Chem. Phys.* **2002**, *117*, 6939.
[38] C. Hättig, *J. Chem. Phys.* **2003**, *118*, 7751.
[39] Gaussian 03, Revision A.1, M. J. Frisch, G. W. Trucks, H. B. Schlegel, G. E. Scuseria, M. A. Robb, J. R. Cheeseman, J. A. Montgomery, Jr., T. Vreven, K. N. Kudin, J. C. Burant, J. M. Millam, S. S. Iyengar, J. Tomasi, V. Barone, B. Mennucci, M. Cossi, G. Scalmani, N. Rega, G. A. Petersson, H. Nakatsuji, M. Hada, M. Ehara, K. Toyota, R. Fukuda, J. Hasegawa, M. Ishida, T. Nakajima, Y. Honda, O. Kitao, H. Nakai, M. Klene, X. Li, J. E. Knox, H. P. Hratchian, J. B. Cross, C. Adamo, J. Jaramillo, R. Gomperts, R. E. Stratmann, O. Yazyev, A. J. Austin, R. Cammi, C. Pomelli, J. W. Ochterski, P. Y. Ayala, K. Morokuma, G. A. Voth, P. Salvador, J. J. Dannenberg, V. G. Zakrzewski, S. Dapprich, A. D. Daniels, M. C. Strain, O. Farkas, D. K. Malick, A. D. Rabuck, K. Raghavachari, J. B. Foresman, J. V. Ortiz, Q. Cui, A. G. Baboul, S. Clifford, J. Cioslowski, B. B. Stefanov, G. Liu, A. Liashenko, P. Piskorz, I. Komaromi, R. L. Martin, D. J. Fox, T. Keith, M. A. Al-Laham, C. Y. Peng, A. Nanayakkara, M. Challacombe, P. M. W. Gill, B. Johnson, W. Chen, M. W. Wong, C. Gonzalez, and J. A. Pople, Gaussian, Inc., Pittsburgh, PA (2003).
[40] W. L. Meerts, M. Schmitt, G. Groenenboom, *Can. J. Chem.* **2004**, *82*, 804.
[41] W. L. Meerts, M. Schmitt, *Phys. Scr.* **2006**, *73*, C47.
[42] W. L. Meerts, M. Schmitt, *Int. Rev. Phys. Chem.* **2006**, *25*, 353.

[43] M. Schmitt, W. L. Meerts, in *Handbook of High Resolution Spectroscopy* (Eds.: M. Quack, F. Merkt), Wiley, Hoboken, **2011**.

[44] A. Ostermeier, A. Gawelcyk, N. Hansen, in *Parallel Problem Solving from Nature, PPSN III* (Eds.: Y. Davidor, H.-P. Schwefel, R. Männer), Springer, Berlin, Heidelberg, **1994**.

[45] N. Hansen, A. Ostermeier, *Evolutionary Comput.* **2001**, *9*, 159.

[46] J. Wilke, M. Wilke, W. L. Meerts, M. Schmitt, *J. Chem. Phys.* **2016**, *144*, 044201.

[47] S. Gerstenkorn, P. Luc, *Atlas du spectre d'absorption de la molécule d'iode 14800 – 20000 cm^{-1}*, CNRS, Paris, **1986**.

[48] M. Schmitt, *Spektroskopische Untersuchungen an Wasserstoffbrückenbindungen*, Habilitation, Heinrich-Heine-Universität, Math. Nat. Fakulat, Düsseldorf, 2000.

[49] M. Schmitt, J. Küpper, D. Spangenberg, A. Westphal, *Chem. Phys.* **2000**, *254*, 349.

[50] L. S. Prabhumirashi, D. K. N. Kutty, A. S. Bhide, *Spectrochim. Acta Part A* **1983**, *39*, 663.

[51] O. Desyatnyk, L. Pszczolkowski, S. Thorwirth, T. M. Krygowskid, Z. Kisiel, *Phys. Chem. Chem. Phys.* **2005**, *7*, 1708.

[52] H. C. Allen, P. C. Cross, *Molecular Vib-Rotors*, Wiley, New York, **1963**.

[53] T. M. Korter, D. R. Borst, C. J. Butler, D. W. Pratt, *J. Am. Chem. Soc.* **2001**, *123*, 96.

[54] D. R. Borst, Ph.D. Thesis, University of Pittsburgh, Pittsburgh, 2001.

[55] J. A. Reese, T. V. Nguyen, T. M. Korter, D. W. Pratt, *J. Am. Chem. Soc.* **2004**, *126*, 11387.

[56] D. R. Borst, T. M. Korter, D. W. Pratt, *Chem. Phys. Lett.* **2001**, *350*, 485.

[57] J. R. Platt, *J. Chem. Phys.* **1949**, *17*, 484.

[58] E. Heilbronner, J. Murrell, *Mol. Phys.* **1968**, *6*, 1.